

Understanding adsorption of hydrogen atoms on graphene

Simone Casolo

University of Oslo, Department of Physics, P.O.Box 1048 Blindern, NO-0316 Oslo, Norway. On leave from Dept. of Physical Chemistry and Electrochemistry, University of Milan

Ole Martin Løvvik

University of Oslo, Department of Physics, P.O.Box 1048 Blindern, NO-0316 Oslo, Norway and SINTEF Materials and Chemistry, Forskningsvn 1, NO-0314 Oslo, Norway

Rocco Martinazzo

*Dept. of Physical Chemistry and Electrochemistry and CIMAINA, University of Milan, V. Golgi 19, 20133 Milan, Italy**

Gian Franco Tantardini

Dept. of Physical Chemistry and Electrochemistry and CIMAINA, University of Milan, V. Golgi 19, 20133 Milan, Italy and ISTM Institute for Molecular Science and Technology, V. Golgi 19, 20133 Milan, Italy

Adsorption of hydrogen atoms on a single graphite sheet (graphene) has been investigated by first-principles electronic structure means, employing plane-wave based, periodic density functional theory. A reasonably large 5×5 surface unit cell has been employed to study single and multiple adsorption of H atoms. Binding and barrier energies for sequential sticking have been computed for a number of configurations involving adsorption on top of carbon atoms. We find that binding energies per atom range from ~ 0.8 eV to ~ 1.9 eV, with barriers to sticking in the range $0.0 - 0.2$ eV. In addition, depending on the number and location of adsorbed hydrogen atoms, we find that magnetic structures may form in which spin density localizes on a $\sqrt{3}\times\sqrt{3}R30^\circ$ sublattice, and that binding (barrier) energies for sequential adsorption increase (decrease) linearly with the site-integrated magnetization. These results can be rationalized with the help of the valence-bond resonance theory of planar π conjugated systems, and suggest that preferential sticking due to barrierless adsorption is limited to formation of hydrogen pairs.

I. INTRODUCTION

Recent years have witnessed an ever growing interest in carbon-based materials. Carbon, being a small atom with a half-filled shell, is able to mix its valence s and p orbitals to various degrees, thereby forming the building block for extended structures of incredibly different electronic, magnetic and mechanical properties. Among them, those formed by sp^2 C atoms have attracted much attention in the last few years. They can be collectively termed as graphitic compounds and comprise graphite, carbon nanotubes, fullerenes, Polycyclic Aromatic Hydrocarbons (PAHs), and recently graphene (the one-atom thick layer of graphite) and graphene nanoribbons (GNRs). In particular, the revolutionary (and embarrassing simple) fabrication of graphene (Novoselov et al., 2004) has opened the way for a wealth of studies in both fundamental and applied science. New, extraordinary properties have become available to material design since its isolation. Indeed, even though they have been known since the first theoretical analysis by Wallace (Wallace, 1947), it was only the experimental observation of the ex-

istence of one-atom thick layer of graphite that triggered much of the current interest. In particular, one of the most interesting aspects of graphene is that it presents low energy excitations as massless, chiral, Dirac fermions mimicking the physics of quantum electrodynamics (Novoselov et al., 2005; Zhang et al., 2005; Castro Neto et al., 2008).

In this context, adsorption of hydrogen atoms on graphene and GNRs can be used to tailor electronic and magnetic properties, as already suggested for other 'defects', with the advantage of being much easier to realize than e.g. vacancies. In addition, interaction of hydrogen atoms with graphitic compounds has been playing an important role in a number of fields as diverse as nuclear fusion (Meregalli and Parrinello, 2001; Mayer et al., 2001), hydrogen storage (Schlapbach and Züttel, 2001) and interstellar chemistry (Hartquist and Williams, 1999).

In material design for hydrogen storage, several carbon based structures has been proposed as candidates (Schlapbach and Züttel, 2001), in particular in connection with the spillover effect following embedding of metallic nanoparticles. Though these materials are in practice still far from the weight percent target stated by the US department of Energy, they remain a cheap and safe alternative, and a deeper understanding of the mechanisms underlying adsorption may lead

*Electronic address: rocco.martinazzo@unimi.it

in future to a more efficient material design.

In interstellar chemistry hydrogen-graphite and hydrogen-PAHs systems have become realistic models to investigate molecular hydrogen formation in the interstellar medium (ISM). There are still open questions in this context since, in spite of continuous destruction by UV radiation and cosmic rays, H_2 is the most abundant molecule of the ISM. It is now widely accepted that H_2 can only form on the surface of interstellar dust grains and particles (Gould and Salpeter, 1963; Hollenbach and Salpeter, 1970, 1971), which - with the exception of cold, dense molecular clouds- are either carbon-coated silicate grains or carbonaceous particles or large PAHs (Greenberg, 2002; Williams and Herbst, 2002; Draine, 2003). This finding has stimulated a number of theoretical (Jeloaica and Sidis, 1999; Sha and Jackson, 2002; Sha et al., 2002; Zecho et al., 2002; Sha et al., 2005; Morisset et al., 2004; Allouche et al., 2005; Morisset et al., 2005; Martinazzo and Tantardini, 2005; Allouche et al., 2006; Kerwin et al., 2006; Martinazzo and Tantardini, 2006a,b; Bonfanti et al., 2007; Cuppen and Hornekær, 2008; Medina and Jackson, 2008) and experimental (Zecho et al., 2002; Güttler et al., 2004a; Zecho et al., 2004; Güttler et al., 2004b; Andree et al., 2006; Hornekær et al., 2006a,b; Baouche et al., 2006; Creighan et al., 2006; Islam et al., 2007; Hornekær et al., 2007) studies on hydrogen graphitic systems aimed at elucidating the possible reaction pathways leading ultimately to molecule formation.

One interesting finding of these studies is the tendency of hydrogen atoms to cluster at all but very low coverage conditions (Andree et al., 2006; Hornekær et al., 2006a,b, 2007). New mechanisms for hydrogen sticking (Hornekær et al., 2006b) and new recombination pathways (Hornekær et al., 2006a) have been proposed, based on the now common agreement that the presence of one or more adsorbate atoms strongly influences subsequent adsorption. It is clear that such an influence can only result as a consequence of a substrate-mediated interaction which makes use of the unusual electronic properties of graphitic compounds, but at present a comprehensive model for multiple chemisorption is still missing.

In this work we present first principles calculations of single and multiple adsorption of hydrogen atoms on a graphene sheet, used as a model graphitic material, with the aim of understanding the relationship between the substrate electronic properties and the stability of various cluster configurations. This work parallels analogous investigations of defects in graphene and GNRs (Pereira et al., 2006; Yazyev and Helm, 2007; Pisani et al., 2008; Pereira et al., 2008; Palacios et al., 2008; Yazyev, 2008). Indeed, they all share the disappearance of one or more carbon p orbitals from the $\pi - \pi^*$ band system, a fact which may lead to the appearance of magnetic textures and introduce site-specific dependence on the chemical prop-

erties. Complementing previous investigations, however, we show how the simple π resonance chemical model helps in rationalizing the findings. A parallel work on different graphitic substrates (PAHs) will follow shortly (Bonfanti et al., 2008).

The paper is organized as follows. Details of our first-principles calculations are given in Section II, and their results in Section III, where we analyze adsorption of a single H atom and briefly introduce the chemical model (Section III.A), we consider formation of pairs (Section III.B) and formation of three- and four-atom clusters (Section III.C). We summarize and conclude in Section IV.

II. COMPUTATIONAL METHODS

Periodic density functional theory as implemented in the Vienna *Ab initio* Simulation Package suite (VASP) (Kresse and Hafner, 1994, 1993; Kresse and Furthmüller, 1996a,b) has been used in all the calculations. The projector-augmented wave method within the frozen core approximation has been used to describe the electron-core interaction (Blöchl, 1994; Kresse and Joubert, 1999), with a Perdew-Burke-Ernzerhof (PBE) (Perdew et al., 1996, 1997) functional within the generalized gradient approximation (GGA). Due to the crucial role that spin plays in this system all our calculations have been performed in a spin unrestricted framework.

All calculations have used an energy cutoff of 500 eV and a $6 \times 6 \times 1$ Γ -centered k -points mesh to span the electron density, in a way to include all the special points of the cell. The linear tetrahedron method with Blöchl corrections is used (Blöchl et al., 1994) together with a 0.2 eV smearing. All the atomic positions have been fully relaxed until the Hellmann-Feynman forces dropped below 10^{-2} eV \AA^{-1} , while convergence of the electronic structures has been ensured by forcing the energy difference in the self consistent cycle to be below 10^{-6} eV, with the exception of energy barriers determination where the thresholds were 10^{-5} eV for electrons and 10^{-4} eV for ions. We have checked that both setups give the same results within a meV accuracy.

The slab-supercell considered has been carefully tested and a 20 \AA vacuum along the c axis has been adopted to ensure no reciprocal interaction between periodical images. We find that using the above settings the interaction between two adjacent graphite layers is ~ 2 meV, largely within the intrinsic DFT error. This result is in agreement with literature data (Hasegawa and Nishidate, 2004; Rydberg et al., 2003). For this reason a single graphene sheet can also model the Bernal (0001) graphite surface, at least as long as chemical interactions are of concern.

The cell size on the surface plane is a fundamental parameter for these calculations, since we have found

unit cell	θ / ML	d_{puck} / Å		E_{chem} / eV	
		this work	others	this work	others
2x2	0.125	0.36	0.36 ¹	0.75	0.67 ¹
3x3	0.062	0.42	0.41 ²	0.77	0.76 ²
cluster	0.045	-	0.57 ³	-	0.76 ³
4x4	0.031	0.48	-	0.79	0.76 ⁴ , 0.85 ⁵
5x5	0.020	0.59	-	0.84	0.71 ⁶ , 0.82 ⁷
8x8	0.008	-	-	-	0.87 ⁸

Table I Chemisorption energy (E_{chem}) and equilibrium height of the C atom above the surface (d_{puck}) for H adsorption on top of a C atom, for a number of surface unit cells, corresponding to different coverages θ . Ref. 1 Sha and Jackson (2002), Ref. 2 Kerwin and Jackson (2008), Ref. 3 Ferro et al. (2003), Ref. 4 Duplock et al. (2004), Ref. 5 Hornekær et al. (2006b), Ref. 6 Roman et al. (2007), Ref. 7 Chen et al. (2007), Ref. 8 Lethinen et al. (2004).

that chemisorption energies strongly depend on the coverage (see below). We choose to use a reasonably large 5x5 cell in order to get some tens of meV accuracy while keeping the computational cost as low as possible. Even with this size, however, the possibility of interactions between images has always to be taken into account when rationalizing the data.

III. RESULTS

A. Single atom adsorption

Chemisorption of single H atoms on graphite has long been studied since the works of Jeloica and Sidis (1999) and Sha and Jackson (2002), who first predicted surface reconstruction upon sticking. Such a reconstruction, i.e. the puckering of the carbon atom beneath the adsorbed hydrogen atom, occurs as a consequence of $sp^2 - sp^3$ rehybridization of the valence C orbitals needed to form the σ CH bond. Since this electronic/nuclear rearrangement causes the appearance of an energy barrier ~ 0.2 eV high, sticking of hydrogen atoms turns out to be a thermally activated process which hardly occurs at and below room temperature (Kerwin and Jackson, 2008).

As already said in Section II, we have re-considered adsorption of single hydrogen atoms for different sizes of the surface unit cell. We have found that both the binding energy and the puckering height are strongly affected by the size of the unit cell (see Table I), and even the results of the 5x5 cell turns out to be in error of about ~ 30 meV with respect to the isolated atom limit estimated by the calculation at 0.008 ML coverage (Lethinen et al., 2004). In particular, we have found that some cautions is needed in comparing the height of the carbon atom involved in the bond since constraining the neighboring carbon atoms in geometry optimization may lead to considerable surface

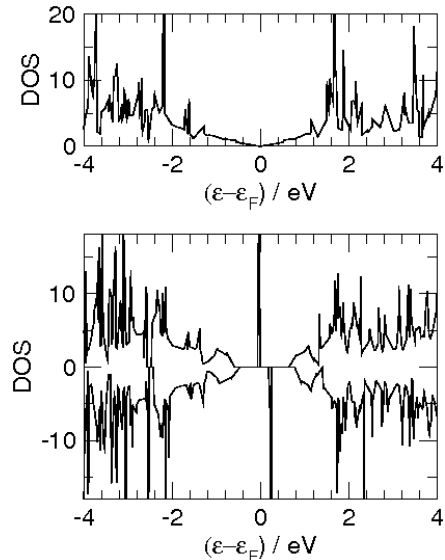


Figure 1 Top panel: total density of states for graphene. Bottom panel: density of states for spin-up (positive values) and spin-down (negative values) components in a 5x5 H layer on graphene.

strain.

Despite this, we have consistently used the 5x5 cell in studying multiple adsorption of hydrogen atoms. Indeed, this size allowed us to investigate a number of stable configurations involving two, three and four adsorbed H atoms, along with the barrier to their formation, with the same set-up described in Section II. Interactions between images do indeed occur for some configurations but, as we show below, this does not prevent us to get a clear picture of the adsorption processes we are interested in.

In agreement with previous studies we find that hydrogen adsorption can only occur if the substrate is allowed to relax. Without relaxation the adsorption curves on different surface sites are repulsive, and only a metastable minimum is found for the atop position (Sha and Jackson, 2002). Surface relaxation requires about 0.8 – 0.9 eV and results in the outward motion of the carbon atom forming the CH bond (see Table I and Jeloica and Sidis (1999); Sha and Jackson (2002)).

In addition, we have investigated the electronic substrate properties of the resulting hydrogenated graphene, in order to get hints for understanding the adsorption process of additional atoms. In Fig. 1 we show the Density of States (DOS) of the 5x5 H-graphene equilibrium structure (bottom panel), compared to that of clean graphene (top panel). It is evident from the figure that hydrogen adsorption causes the appearance of a double peak in the DOS, symmetrically placed around the Fermi level. This is in agreement with rigorous results that can be obtained in tight binding theory for *bipartite* lattices. Indeed, Inui et al. (1994) have shown that for a bipartite lat-

tice with n_A A lattice sites and n_B B lattice sites a sufficient condition for the existence of mid-gap states is a lattice imbalance ($n_A \neq n_B$). In particular, there exist $n_I = |n_A - n_B|$ mid-gap states with *vanishing* wavefunction on the minority lattice sites. In H-graphene a lattice imbalance results as a consequence of the bond with the H atom which makes one of p orbitals no longer available for taking part to the $\pi - \pi^*$ band system. There is one mid-gap state for each spin species, and the degeneracy is lifted if exchange-correlation effects are taken into account, as shown in Fig.1 for our DFT results. This state has been mapped out in Fig.2 (left panel), where we report a contour map of the spin density at a constant height 0.47 \AA above the surface. It is clear from the figure that if adsorption occurs on a A lattice site the spin-density (due to mainly to the above mid-gap state) localizes on B lattice sites. The latter now contain most of the $1 \mu_B$ magnetization ($\mu_B = \text{Bohr magneton}$) previously carried by the H atom species, and a slight spin-down excess on A sites results as a consequence of the spin-polarization of the lower lying states. This is made clearer in the right panel of Fig. 2 where we report the spin-density at the same height above the surface as before along a rectilinear path joining a number of C atom sites away from the adsorption site (see Fig.5 for the labels). Note that the spin-density decays only slowly with the distance from the adsorption site, in agreement with theoretical results that suggest that in the case of two dimensional graphene this decay corresponds to a non-normalizable state with a $1/r$ tail (in contrast to non-zero gap substrates such as armchair nanoribbons where mid-gap states are normalizable)(Pereira et al., 2006). With our unit cell the effect of the interaction with the images is already evident at rather short distances, but as we show below, this effect has no influence on the interpretation of the results. Note also that this spin pattern is common to other ‘defects’ (e.g. vacancies, voids and edges) which have been known for some time to strongly modify the electronic properties of graphene and graphene-like structures, and to (possibly) produce long-range ordered magnetic structures (Pereira et al., 2006; Yazyev and Helm, 2007; Pisani et al., 2008; Pereira et al., 2008; Palacios et al., 2008; Yazyev, 2008; Lethinen et al., 2004; Mizes and Foster, 1989; Ruffieux et al., 2000; Kusakabe and Maruyama, 2003; Jiang et al., 2007; Yazyev et al., 2008; Yazyev and Katsnelson, 2008). In particular, in a recent, comprehensive study, Palacios *et al.*, using a mean-field Hubbard model for graphene, have clarified the appearance of magnetic textures associated to vacancies and predicted the emergence of magnetic order (Palacios et al., 2008). Their model also suits well to ‘defects’ such as the presence of the adsorbed hydrogen atoms.

From a chemical point of view the above spin pattern (and the resulting magnetic properties) arise from the ‘spin-alternation’ typical of π conjugated com-

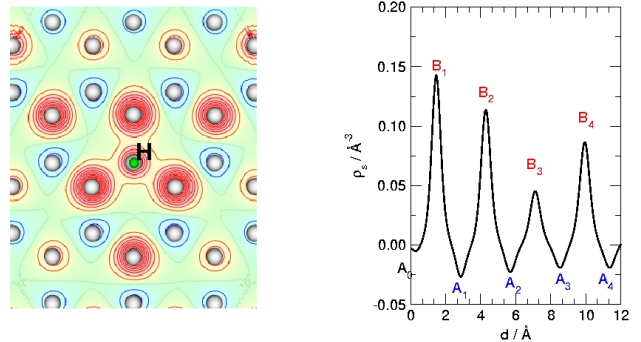


Figure 2 Spin density 0.47 \AA above the graphene surface after adsorption of a hydrogen atom. Left: contour map with red/blue lines for spin-up/spin-down excess respectively. Right: spin-density at the same height as on the left panel, along a path joining the C atoms (for the labels see Fig.5).

pounds. This behavior is easily understood in terms of resonant chemical structures, such as those shown in Fig.3 for a coronene molecule. In this and analogous Polycyclic Aromatic Hydrocarbons (PAHs), the π electron system can be described as a resonant combination of conventional, alternated double bond structures, like the one shown in the upper panel of Fig.3 (see *a*). Once a hydrogen atom has been adsorbed on the surface, an unpaired electron is left on one of the neighboring C atoms (*b*, left panel), which can subsequently move in each of the carbon atoms belonging to a sublattice $\sqrt{3}x\sqrt{3}R30^\circ$ by ‘bond-switching’ (see *b,c*). Spin-alternation arises from the ‘resonant’ behavior of an unpaired electron in α position (the nearest neighbor one) with respect to a double bond: such ‘resonance’ can be naively viewed as the spin re-coupling of the unpaired electron with the electron on the neighboring site, a process which sets free a second electron on the same sublattice.

This picture, despite its embarrassing simplicity, can be put on firm grounds in the context of the Valence Bond (VB) theory of chemical bonding (see e.g. Raimondi et al. (1985); Cooper et al. (1987); Gerratt et al. (1997); Li and McWeeny (2002); Cooper (2002)). Focusing on the π electron system, this can be done with the help of a simple (correlated) VB *ansatz* for the N electron wavefunction of the π cloud, namely

$$\Psi_{SN} = \mathcal{A}(\phi_1\phi_2..\phi_N\Theta_{SN}) \quad (1)$$

where \mathcal{A} is the antisymmetric projector, $\phi_i = \phi_i(\mathbf{r})$ for $i = 1, N$ are (spatial) orbitals accommodating the N electrons, and Θ_{SN} is a N electron spin-function with spin quantum number S . The latter is usually variationally optimized by expansion on a spin function basis,

$$\Theta_{SN} = \sum_{k=1, f_S^N} c_k \Theta_{SN;k}$$

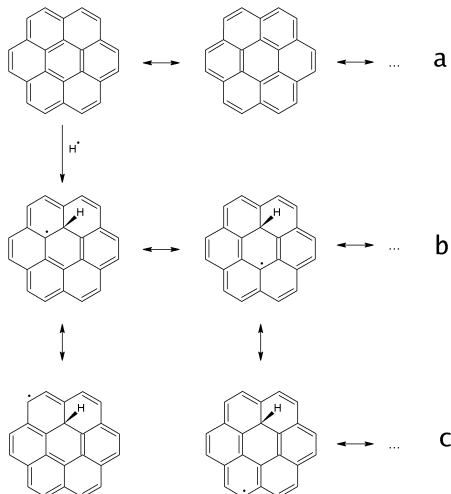


Figure 3 (a) The π resonating chemical model for a graphenic surrogate (coronene). (b), (c) Spin-alternation after hydrogen adsorption.

where f_s^N is the dimension of the spin-subspace of eigenfunctions of \mathbf{S}^2 with eigenvalue $S(S+1)$ and given magnetization¹. Among these basis-functions the ‘perfect pairing’ set devised by Rumer, though non-orthogonal, is chemically appealing since for a given S and $M_s = S$ the total magnetization is given by $2S$ electrons coupled at high spin, the remaining $N - 2S$ being accommodated in $(N - 2S)/2$ singlet-coupled pairs (see Simonetta et al. (1968)). Then, if the orbitals ϕ_i are *localized* on the atoms, the resulting wavefunction

$$\Psi_{SN} = \sum_{k=1, f_s^N} c_k \mathcal{A}(\phi_1 \phi_2 \dots \phi_N \Theta_{SN;k}) = \sum_{k=1, f_s^N} c_k \Psi_{SN;k}$$

is a superposition of conventional ‘structures’ $\Psi_{SN;k}$ describing pairs of atom-centered, singlet-coupled orbitals (i.e. Lewis chemical bonds and lone pairs) and unpaired electrons. ‘Classical’ molecules require just one perfect-pairing spin function coupling those pairs of orbitals with substantial overlap. Less conventional molecules, such as π conjugated systems, need a true superposition of two or more spin structures, since the energy gain (also known as *resonance* energy) in allowing such superposition is particularly important in these cases. Correspondingly, the classical Lewis picture of chemical bonds is extended to account for the resonance phenomenon, as shown in Fig. 3 with double ended arrows indicating *superposition* of chemical structures.

¹ f_s^N is given by the expression $f_s^N = N!/(N/2+S+1)!(N/2-S)!(2S+1)$ and does not depend on the value M_s of the spin-projection $\hat{\mathbf{z}}\mathbf{S}$ along the axis $\hat{\mathbf{z}}$, since these subspaces are isomorphic to each other.

Early applications of the theory, starting from the landmark work of Heitler and London, used *frozen* atomic orbitals. In modern, *ab initio* use of the theory both the spin-coupling coefficients c_k and the orbitals can be variationally optimized, even when using a number of configurations in place of the single orbital product appearing in eq.(1) (see e.g. Li and McWeeny (2002)), in close analogy to what is done in molecular orbital theory with the MultiConfiguration Self-Consistent Field (MCSCF) approach. The interesting thing is that these optimized orbitals, as a consequence of electron correlation, are usually (if not always) localized on atomic centers and are only slightly polarized by the environment (Cooper et al., 1987; Gerratt et al., 1997; Cooper et al., 1991), thereby supporting the interpretation of the simple wavefunction of eq.(1) as a quantum-mechanical translation of Lewis theory of chemical bond. This is true, in particular, for the benzene molecule, the prototypical π resonant system, where six, p -like orbitals are mostly coupled by two, so-called Kekulé structures (Cooper et al., 1987; Tantardini et al., 1977; Cooper et al., 1986)².

From a physical point of view, wavefunction (1) generalizes to N electron systems the Heitler-London *ansatz* forming the basis for the Heisenberg model of magnetism in insulators. In addition, if the orbitals are allowed to be ‘polarized’, band-like behavior can be accommodated, along with collective spin excitation, as in the Hubbard model (Hubbard, 1963) which has been finding widespread use in investigating graphitic compounds. The fact that Hubbard model, and its Heisenberg limit, can be derived by suitable approximations to Valence-Bond *ansatz* has long been known in the chemical literature, especially in connection to π resonant systems (see e.g. Wu et al. (2002, 2003) and references therein. Hubbard model is also known as Pariser-Parr-Pople model in the chemical literature, after Pariser and Parr (Pariser and Parr, 1953a,b) and after Pople (Pople, 1953)). We can roughly say that Heisenberg models correspond to the ‘classical’ valence theory developed by Heitler, London, Pauling and Van Vleck in the twenties which put the basis for explaining chemical bond using *frozen* atomic orbitals, whereas Hubbard models arise from the modern version of theory, started with Coulson and Fisher and pushed forward by Gerratt and others, who used ‘polarizable’ orbitals in the same spin scheme set up in the original theory (Cooper et al.,

² For $S = 0$ and $N = 6$ the set of five linearly independent Rumer structures is given by two Kekulé structures and the three additional ‘Dewar’ structures. A resonance energy $\simeq 0.8$ eV can be computed when using two Kekulé structures in place of one, whereas only some tenths of meV are gained when full optimization of the spin function is performed (Bonfanti et al., 2008).

1987, 1986).

In the following Sections, we will use the above wavefunction (eq.(1)) as a simple guide to interpret the results of our first-principles calculations, keeping in mind its connections with the traditional chemical picture on the one hand and the Hubbard model on the other. As we will show in the following, even at this qualitative level, a number of useful insights can be gained from such a picture. As a first example we can reconsider adsorption of a single hydrogen atom on graphene. In a diabatic picture (i.e. when constraining the spin-coupling to the Kekulé structures of Fig.3, panel a) the interaction between graphene and the incoming H atom is expected to be repulsive, since no electron is available to form the CH bond. On the other hand, a low lying spin-excited state corresponding to a Dewar-like structure (which has two, singlet-paired electrons on opposite, no-overlapping end of a benzene ring) would give rise to an attractive, barrierless interaction. At short-range, then, an avoided crossing between the two doublet curves occurs which signals the spin-transition leading to bond formation, even though this can lead only to a metastable state if surface reconstruction is not allowed, as indeed found in DFT calculations (e.g. see Fig. 2 in (Sha and Jackson, 2002)). Actually, in this case the situation is a bit more complicated since a slightly lower-lying state in the triplet manifold (obtained by spin-flipping the above spin-excited Dewar-like structure) contributes to the same doublet manifold. Valence Bond calculations on the simpler benzene-H system confirms this picture (Bonfanti et al., 2008), see Fig.4.

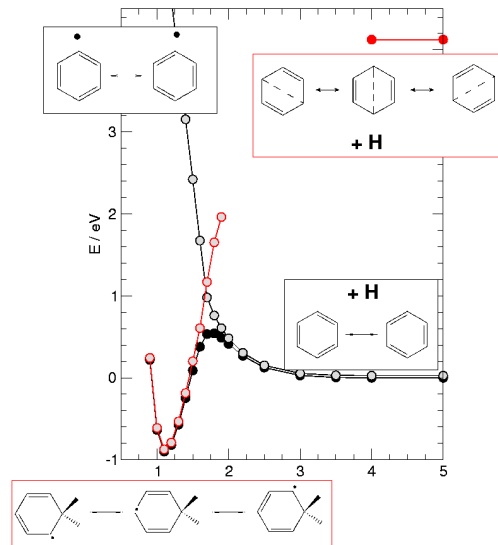


Figure 4 Interpretation of the sticking barrier as an avoided crossing between chemical structures. Valence bond results for the benzene-H system, from Ref. (Bonfanti et al., 2008). Solid black and red circles for the ground ($C_6H_6(^1A_{1g}) + H(^2S)$) and the first excited states ($C_6H_6(^3B_{1u}) + H(^2S)$), as obtained at the single-orbital-string level of eq.1, with orbital optimization. Quasidiabatic results are obtained by properly constraining the spin space: Kekulé structures only (lower right and upper left insets) for empty black circles; structures in the lower left inset for empty red circles. Also shown in the upper right inset the main (Dewar-like) structures needed to described the $^3B_{1u}$ state of benzene.

B. Secondary adsorption

Next we consider adsorption of a second atom on the different sites $A(n)$ ($n = 1, 6$) and $B(n)$ ($n = 1, 6$) shown in Fig.5, with a first adsorbed H atom on site $A(0)$. For each site we have investigated the ground spin manifold by allowing full relaxation of the magnetization. In addition, in most of the cases, we have also performed magnetization-constrained calculations in order to get insights on both the singlet and the triplet states arising from the interaction between the doublet H-graphene ground-state and the second H atom

The results for the binding energies are reported in Table II, along with the site-integrated magnetizations (M_{SI}) and the total magnetization M . Site-integrated spin-densities have been obtained by integrating the spin-density on a small cylinder (of radius half of the C-C distance in the lattice) centered on each site, and can be considered a rough measure of the total spin excess available on the site. This quantity behaves very similar to the spin-density itself, decreasing in magnitude when increasing the distance from the adsorption site, *separately* for each sublattice. Some exceptions

Position	M_{SI} / μ_B	$E_{\text{bind}} / \text{eV}$	M / μ_B	$E_{\text{bind}}^* / \text{eV}$
$B(1)$	0.109	1.934	0	0.933
$A(1)$	-0.019	0.802	2	0.575
$B(2)$	0.085	1.894	0	0.828
$A(2)$	-0.017	0.749	2	0.531
$B(3)$	0.040	1.338	0	0.646
$A(3)$	-0.016	0.747	2	0.570
$B(4)$	0.076	1.674	0	-
$A(4)$	-0.016	0.747	2	0.573
$B(5)$	0.023	1.033	0	0.590
$A(5)$	-0.014	0.749	2	0.531
$B(6)$	0.028	1.110	0	0.545
$A(6)$	-0.015	0.787	2	-

Table II Binding energies (E_{bind}) for secondary adsorption to form the H-pairs shown in Fig.5, along with the site-integrated magnetizations (M_{SI}) before adsorption, and the total ground-state magnetization (M) after adsorption obtained when fully relaxing the magnetization. Also reported the binding energies obtained when the magnetization is constrained to $M = 0, 2\mu_B$ for A and B sites, respectively. See text for details.

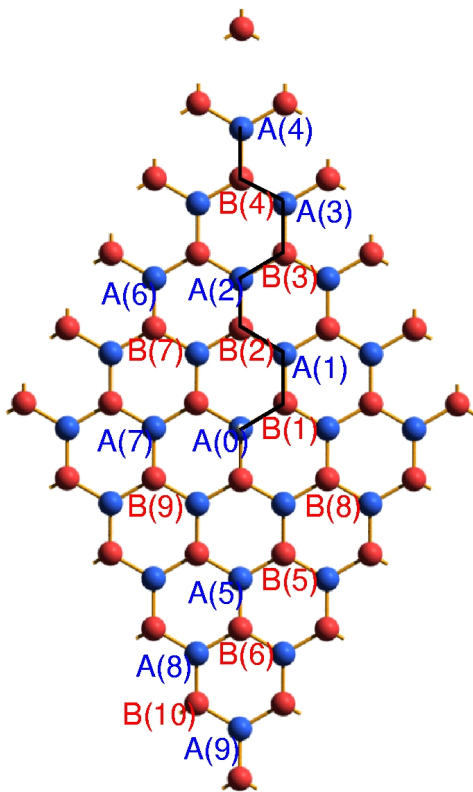


Figure 5 The graphene unit cell used for the calculations with A (blue) and B (red) lattice sites indicated. Also indicated is the path used for Fig.2, A(0) being the first H adsorption site.

are worth noticing, namely the $A(0)$ - $B(5)$ pair, and are due to the cumulative effect of next-neighbors images. Notice, however, that despite their possible artificial nature, results corresponding to any lattice sites when viewed *as a function* of the site-integrated magnetization give insights into the adsorption process.

A quick look at the Table II reveals that the two sublattices A and B behave very differently from each other, as the spin-coupling picture of Fig. 3 (panels *b,c*) suggests. Roughly speaking, adsorption on B lattice is *preferred* over that on the A lattice. The binding energies are much larger than the first adsorption energy reported in Table I (they can be as large as twice the adsorption of the first atom), and give rise to a final unmagnetized state. In contrast, the binding energy for adsorption on a A lattice site is comparable to that of single-H adsorption, and the ground-state of the H-pair on graphene is a triplet ($M=2 \mu_B$).

These findings agree with Lieb's theorem (Lieb, 1989) for the repulsive Hubbard model of a bipartite lattice and a half-filled band, which states that the ground-state of the system has $S = 1/2|n_A - n_B|$. In such model, the electronic state of the system would be described by $N - 2 p$ orbitals (N being the original number of sites), and $n_B = n_A = N/2 - 1$ if adsorp-

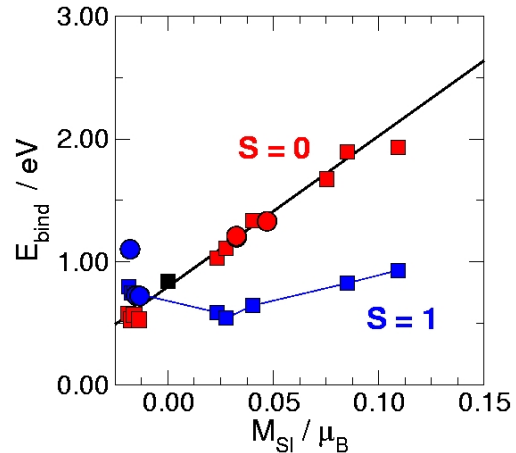


Figure 6 Binding energies for secondary H adsorption as a function of the site-integrated magnetization, for singlet (red squares) and triplet (blue squares) states. Black square is the data point for single H adsorption. Also shown a linear fit to the data set (solid line) and the H binding energy to form some 4-atom clusters from 3-atom ones (red and blue circles for final singlet and triplet states, respectively). See text for details.

tion of the second hydrogen atom proceeds on the B lattice (to form what we can call AB dimers), whereas $n_B = n_A + 2 = N/2$ if it proceeds on the A lattice (to form A_2 dimers). The results are also consistent with the VB framework sketched in Subsection III.A: with reference to Fig. 3 (panels *b,c*), it is clear that when a H atom adsorbs on an B site its electron readily couples with the unpaired electron available on the B sublattice, whereas when adsorption occurs on an A site *two* electrons are left in excess on the B sublattice, and they more favorably couple at high spin.

The relationship between the available unpaired electron density at a given site and the binding energy of adsorbing a second H atom can be made clearer by reporting the energy data of Table II as a function of M_{SI} . This is shown in Fig.6, for both the singlet and triplet states of the dimers, along with the value for the first H adsorption (data point at $M_{SI}=0$). It is clear from the figure that, with the exception of the value for the *ortho*-dimer ($A(0)B(1)$ in Fig.5. This value has been excluded from the linear regression shown in Fig.6), a linear relationship between the binding energy and the site integrated magnetization well describes the situation, and the binding energy for single H adsorption fits well to this picture.

This is again consistent with the chemical model, as long as the site-integrated magnetization is a measure of the unpaired electron density available. According to Section III.A, adsorption of the first hydrogen atom arises from the energy balance between a 'localization energy' (the spin excitation needed to set free an unpaired electron on the given lattice site), the spin-pairing forming the bond, and the surface reconstruction energy. The same is true for adsorption of a

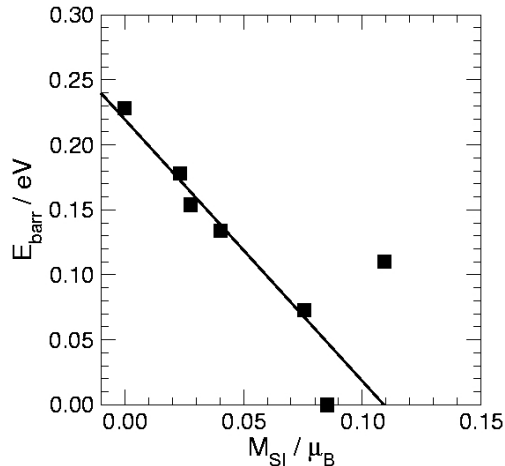


Figure 7 Barrier energies for secondary atom adsorption on the B lattice sites as a function of the site-integrated magnetization. Linear regression of the data omits the values for forming *para* and *ortho* pairs (two rightmost points in the graph).

second atom: localization energy takes only a slightly different form than before because an unpaired electron is already available in one of the two sublattices³, but surface reconstruction energy is *not* expected to depend on the adsorption site. Then, adsorption energies depend on the electronic properties only, and the linear behavior observed for singlet-state dimers in Fig. 6 suggests that the energy needed to localize the unpaired electron on a given site decreases *linearly* when increasing the unpaired electron density available. Notice that negative values of M_{SI} (as found at A sites), correspond to a spin excess *parallel* to that of the incoming H electron, and for these sites localization of an unpaired electron with an *antiparallel* spin requires increasingly more energy when the (magnitude) of the spin-density increases, since this can only be achieved by adding one electron to the site. On the other hand, when a triplet dimer is formed upon adsorption the H electron does *not* make use of the unpaired electron available, and adsorption energies are all around ~ 0.8 eV, i.e. of the order of the first H adsorption. The effect of surface relaxation is only seen in forming the *ortho*-dimer, where few tenths of eV more than the single H relaxation energy are required because of the closeness of the two hydrogen atoms.

Analogous linear behavior can be found when con-

sidering the computed energy barrier to sticking as a function of the site-integrated magnetization, as shown in Fig. 7 for AB dimers. This agrees with the above localization energy and with the common tendency for a linear relationship between the binding and the barrier energies for activated chemical reactions (Brønsted-Evans-Polanyi rule). Exceptions are given by the *ortho*-dimer considered above and by the *para*-dimer ($A(0)B(2)$). The latter, in particular, shows no barrier to adsorption, in agreement to previous theoretical works, and this fact forms the basis of the so-called preferential sticking mechanism. This mechanism was first suggested by Hoernaker *et al.* (Hornekær *et al.*, 2006b) who looked at the STM images formed by exposing Highly Oriented Pyrolytic Graphite (HOPG) samples to a high-energy (1600-2000 K) H atom beam and observed formation of stable pairs, confirmed by first-principles calculations (Hornekær *et al.*, 2006b). Our results suggest that barrierless adsorption on the *para* site is a consequence of both favorable electronic and nuclear factors.

We therefore find that formation of AB dimers is both thermodynamically *and* kinetically favoured over formation of A_2 dimers and single atom adsorption. This agrees with current experimental observations which show evidence for clustering of hydrogen atoms at all but very low ($< 1\%$) coverage conditions. In addition, we notice that the dimers identified so far (Andree *et al.*, 2006; Hornekær *et al.*, 2006a,b) are all of the AB type.

C. Further adsorptions

We consider in this section results concerning formation of cluster of three and four atoms. In these cases, the number of possible configurations is quite large and therefore we limit our analysis to a few important cases. Following analogous notation recently introduced for defects by Palacios *et al.* (2008), we use the ‘chemical formula’ A_nB_m to denote a cluster with n H atoms in the A lattice and m H atoms in the B lattice. According to Lieb’s theorem and to the π resonance picture, we expect that the ground electronic state has $|n - m|$ unpaired electrons. We have considered a number of A_2B_2 , A_2B , A_3B_1 and A_3 clusters, and found that their ground-state has 0, 1, 2 and 3 μ_B of magnetization, respectively, in agreement with the expectation.

Three atom clusters have been obtained by adding one hydrogen atom either to a *para* dimer or to a *meta* dimer, i.e. $A(0)B(2)$ and $A(0)A(1)$ with the labels of Fig.5, respectively. The binding energies of a third hydrogen atom to a *para* dimer structure are reported in Tab.III; since they all are of A_2B type, the total magnetization for the resulting structures is 1 μ_B . A look at Tab.III reveals that adsorption to a third hydrogen atom parallels that of the first H. This is consistent

³ In terms of the wavefunction of eq.(1) this localization energy can be defined by observing that the structures in which the spin-up density localizes on the $(N - 1)$ -th site (N even) correspond to $\Psi = A(\phi_1\phi_2\cdots\phi_{N-1}\Theta_{loc}^{N-1})$, where Θ_{loc}^{N-1} is constrained to have the form $\Theta_{loc}^{N-1} = (c_1\Theta_{0,0}^{N-2} + c_2\Theta_{1,0}^{N-2})\alpha$, whereas the ground-state spin function comprises additional contributions from $\Theta_{1,1}^{N-2}\beta$ structures.

Position	$E_{\text{bind}} / \text{eV}$
A(2)	1.516
B(3)	0.847
A(3)	0.727
B(4) (\equiv A(5))	0.971
A(4) (\equiv B(6))	0.821
B(7)	0.727
B(8)	1.301

Table III Binding energies (E_{bind}) for addition of a third H atom to the *para* dimer structure $A(0)B(2)$ on the sites indicated in the first column (labels from Fig. 5).

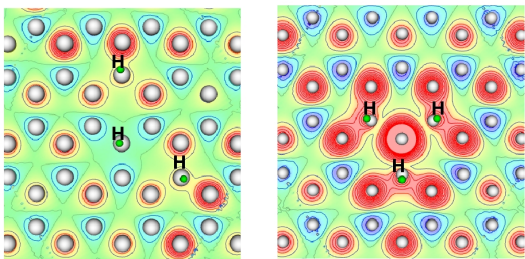


Figure 8 Spin-density 0.40 \AA above the surface for two three-atom clusters. Contour map with red/blue lines for spin-up/spin-down excess respectively. Left and right panel for an A_2B and a A_3 cluster, respectively.

with the π resonance picture, since AB dimers do not have unpaired electrons, and therefore show no preference towards any specific sublattice position. There are of course exceptions, notably the values for adsorption onto $A(2)$ and $B(8)$ lattice sites, and these can be reasonably ascribed to the effect of surface relaxation. Indeed, relaxation energies per atom in ‘compact’ clusters may considerably differ from the value of the single H atom, being always of the order of the binding energies themselves ($\sim 0.8 \text{ eV}$). Similar conclusions hold when adding a third H atom to the (magnetic) *meta* dimer $A(0)A(1)$: adsorption on B lattice sites is strongly favored ($E_{\text{bind}} = 1.2 - 1.9 \text{ eV}$) and produces doublet structures ($M = 1 \mu_B$), whereas H atoms bind to A lattice sites with an energy $\sim 0.7 - 0.8 \text{ eV}$ and produce highly magnetic structures ($M = 3 \mu_B$). Energy barriers to adsorption follow the same trend: preliminary calculations show that, with few exceptions, barriers to sticking a third H atom compare rather well with that for single H atom adsorption for the processes $AB \rightarrow A_2B$ and $A_2 \rightarrow A_3$, and may be considerably smaller for $A_2 \rightarrow A_2B$ ones.

In addition, again consistently with π resonance picture, we found that all the considered 3-atom structures, with one or two unpaired electrons, show an alternation pattern in their spin-density maps. As an example, Fig.8 reports the spin-density maps for

	M_{SI} / μ_B	$E_{\text{bind}} / \text{eV}$	M / μ_B
$B(9)$	-0.0180	1.103	2
$A(7)$	0.0471	1.331	0
$B(6)$	-0.0151	0.727	2
$A(8)$	0.0325	1.210	0
$B(10)$	-0.0134	0.723	2
$A(9)$	0.0326	1.201	0

Table IV Binding (E_{bind}) energies for adsorption to form H-quadruples from the $A(0)B(2)B(8)$ cluster, along with the site-integrated magnetizations (M_{SI}) and the total ground-state magnetization (M), before and after adsorption, respectively. See Fig.5 for atom labels.

an A_2B (left panel) and an A_3 (right panel) cluster. Analogously to Subsection III.B we find that analysis of these spin-density maps gives insights to the adsorption properties of a fourth hydrogen atom. Table IV, for example, reports binding energies to form some 4-atom clusters from the stable $A(0)B(2)B(8)$ one, the final total magnetization of the resulting structures and the values of the corresponding site-integrated magnetization before adsorption. The computed binding energies compare rather well with the dimer values, as can be seen in Fig. 6 where it is clear that the results fit well to the *same* linear trend obtained before. Few exceptions are for compact clusters where substrate relaxation does play some role. With such exceptions in mind, our results suggest that adsorption of hydrogen atoms on magnetic graphitic substrates (such as those obtained by adsorbing an odd number of H atoms), for a given final spin-state, depends on the local spin-density *only*.

IV. SUMMARY AND CONCLUSIONS

In this work we have presented results of extensive first-principles calculations of the adsorption properties of hydrogen atoms on graphite. A number of possible configurations involving one, two, three and four atoms on the surface have been considered and barrier energies have been computed for some of them. We have found that adsorption of hydrogen atoms is strongly related with substrate electronic properties, and used the chemical model of planar π conjugated systems to rationalize the data. The connection between this model and the valence theory of chemical bond on the one hand, and Hubbard models on the other hand, has been emphasized in Section III.A, and used at a qualitative level to rationalize our findings. In this way, one prominent feature of defective graphitic substrates, i.e. the possibility of forming ordered (microscopic) magnetic patterns, turns out to be related to the spin-alternation typical of π resonant systems. We have also invariably found in the cases considered that Lieb’s theorem for

repulsive Hubbard models can be used to predict spin alignment in ground-state graphitic structures.

Adsorption of single H atoms has been known for some time to be an activated process, with an energy barrier to sticking (~ 0.2 eV) high enough to prevent adsorption at ambient conditions. Adsorption of a second atom more favorably occur on the $\sqrt{3}\times\sqrt{3}R30^\circ$ sublattice where spin-density localizes, and may proceed without barrier if it occurs on the so-called *para* site. This preferential sticking has been recently suggested by experimental and theoretical observations (Hornekær et al. (2006a,b)). We extended the latter analysis by considering a large number of possible dimers and found that (i) binding (barrier) energies generally increase (decrease) linearly as a function of the site-integrated magnetization, and (ii) adsorption properties of the *ortho* and *para* sites are slightly at variance with linear trends, thereby suggesting that substrate relaxation plays some role in these cases.

When considering addition of a third atom we found that the adsorption energetics of the incoming H atom is similar to that of the first one (i.e. a barrier ~ 0.2 eV high and a chemisorption well ~ 0.8 eV deep), unless we start with a ‘magnetic’ dimer in which the two atoms are adsorbed in the same sublattice. (These structures, however, are kinetically and thermodynamically unfavored with respect to the unmagnetized *AB* configurations). This is in agreement with the chemical model, which predicts an open-shell configuration for A_2 dimers and a closed-shell one (with partial restoring of the π aromaticity) for *AB* ones. These results, therefore, suggest that preferential sticking alone cannot provide any *catalytic* route to molecular hydrogen formation on graphite.

Finally, we have considered adsorption energetics in forming clusters of four atoms, and re-gained the same picture obtained in forming pairs, namely that adsorption is strongly biased towards the sublattice in which the spin-density localizes. Actually, the resulting energetics fits well to the linear behavior with respect to the site-integrated magnetization already found for dimer formation. Such a linear relationship suggests that the energy needed to localize the unpaired electron on a given lattice site decreases linearly when increasing the site-integrated magnetization, at least in the range of values covered by this study. Interestingly, this behavior suggests that if we were able to tune the magnetization of the substrate we could *control* the adsorption dynamics of H atoms.

Overall our results, consistently with the π resonance picture, suggest that the *thermodynamically* and *kinetically* favored structures are those that minimize sublattice imbalance, i.e. those A_nB_m structures for which $n_I = |n-m|$ is minimum. The latter number n_I is also the number of mid-gap states in single particle spectra which, according to the Hund-like rule provided by Lieb’s theorem (Lieb, 1989), is directly related to the total spin of the system, $S = n_I/2$,

which is therefore at minimum in the favored structures. Notice that however small the S value can be, this result does *not* preclude the existence of local magnetic structures, antiferromagnetically coupled to each other. The case of an *AB* dimer with two atoms very far from each other provides such an example.

References

- K. S. Novoselov, A. K. Geim, S. V. Morozov, D. Jiang, Y. Zhang, S. V. Dubonos, I. V. Gregorieva, and A. A. Firsov, *Science* **306**, 666 (2004).
- P. R. Wallace, *Phys. Rev.* **71**, 622 (1947).
- K. S. Novoselov, A. K. Geim, S. V. S. V. Morozov, D. Jiang, M. I. Katsnelson, I. V. Gregorieva, S. V. Dubonos, and A. A. Firsov, *Nature* **438**, 197 (2005).
- Y. Zhang, Y.-W. Tan, H. L. Stormer, and P. Kim, *Nature* **438**, 201 (2005).
- A. H. Castro Neto, F. Guinea, N. M. R. Peres, K. S. Novoselov, and A. K. Geim, arXiv:0709.1163v2 (2008).
- V. Meregalli and M. Parrinello, *Appl. Phys. A: Mater. Sci. Process.* **72**, 143 (2001).
- M. Mayer, V. Philipps, P. Wienhold, H. H. J. Seggern, and M. Rubel, *J. Nucl. Mater.* **290-293**, 381 (2001).
- L. Schlapbach and A. Züttel, *Nature* **414**, 353 (2001).
- T. W. Hartquist and D. A. Williams, eds., *The molecular astrophysics of stars and galaxies* (Clarendon Press - Oxford, 1999).
- R. J. Gould and E. E. Salpeter, *Astrophys. J.* **138**, 393 (1963).
- D. Hollenbach and E. E. Salpeter, *J. Chem. Phys.* **53**, 79 (1970).
- D. Hollenbach and E. E. Salpeter, *Astrophys. J.* **163**, 155 (1971).
- J. M. Greenberg, *Surf. Sci.* **500**, 793 (2002).
- D. A. Williams and E. Herbst, *Surf. Sci.* **500**, 823 (2002).
- B. T. Draine, *Annu. Rev. Astron. Astrophys.* **41**, 241 (2003).
- L. Jeloica and V. Sidis, *Chem. Phys. Lett.* **300**, 157 (1999).
- X. Sha and B. Jackson, *Surf. Sci.* **496**, 318 (2002).
- X. Sha, B. Jackson, and D. Lemoine, *J. Chem. Phys.* **116**, 7158 (2002).
- T. Zecho, A. Güttler, X. Sha, B. Jackson, and J. Küppers, *J. Chem. Phys.* **117**, 8486 (2002).
- X. Sha, B. Jackson, D. Lemoine, and B. Lepetit, *J. Chem. Phys.* **122**, 014709 (2005).
- S. Morisset, F. Aguillon, M. Sizun, and V. Sidis, *J. Chem. Phys.* **121**, 6493 (2004).
- A. Allouche, Y. Ferro, T. Angot, C. Thomas, and J.-M. Layet, *J. Chem. Phys.* **123**, 124701 (2005).
- S. Morisset, F. Aguillon, M. Sizun, and V. Sidis, *J. Chem. Phys.* **122**, 194702 (2005).
- R. Martinazzo and G. F. Tantardini, *J. Phys. Chem. A* **109**, 9379 (2005).
- A. Allouche, A. Jelea, F. Marinelli, and Y. Ferro, *Phys. Scr.* **T124**, 91 (2006).
- J. Kerwin, X. Sha, and B. Jackson, *J. Phys. Chem. B* **110**, 18811 (2006).
- R. Martinazzo and G. F. Tantardini, *J. Chem. Phys.* **124**, 124702 (2006a).

- R. Martinazzo and G. F. Tantardini, *J. Chem. Phys.* **124**, 124703 (2006b).
- M. Bonfanti, R. Martinazzo, G. F. Tantardini, and A. Ponti, *J. Phys. Chem. C* **111**, 5825 (2007).
- H. Cuppen and L. Hornekær, *J. Chem. Phys.* **128**, 174707 (2008).
- Z. Medina and B. Jackson, *J. Chem. Phys.* **128**, 114704 (2008).
- A. Güttler, T. Zecho, and J. Küppers, *Chem. Phys. Lett.* **395**, 171 (2004a).
- T. Zecho, A. Güttler, and J. Küppers, *Carbon* **42**, 609 (2004).
- A. Güttler, T. Zecho, and J. Küppers, *Surf. Sci.* **570**, 218 (2004b).
- A. Andree, M. Le Lay, T. Zecho, and J. Küppers, *Chem. Phys. Lett.* **425**, 99 (2006).
- L. Hornekær, Ž. Šljivačanin, W. Xu, R. Otero, E. Rauls, I. Stensgaard, E. Lægsgaard, B. Hammer, and F. Besenbacher, *Phys. Rev. Lett.* **96**, 156104 (2006a).
- L. Hornekær, E. Rauls, W. Xu, Ž. Šljivačanin, R. Otero, I. Stensgaard, E. Lægsgaard, B. Hammer, and F. Besenbacher, *Phys. Rev. Lett.* **97**, 186102 (2006b).
- S. Baouche, G. Gamborg, V. V. Petrunin, A. C. Luntz, A. Bauricher, and L. Hornekær, *J. Chem. Phys.* **125**, 084712 (2006).
- S. C. Creighan, J. S. Perry, and S. D. Price, *J. Chem. Phys.* **124**, 114701 (2006).
- F. Islam, E. R. Latimer, and S. D. Price, *J. Chem. Phys.* **127**, 064701 (2007).
- L. Hornekær, W. Xu, R. Otero, T. Zecho, E. Lægsgaard, and F. Besenbacher, *Chem. Phys. Lett.* **446**, 237 (2007).
- V. M. Pereira, F. Guinea, J. Lopes dos Santos, N. Peres, and A. Castro Neto, *Phys. Rev. Lett.* **96**, 036801 (2006).
- O. V. Yazyev and L. Helm, *Phys. Rev. B* **75**, 125408 (2007).
- L. Pisani, B. Montanari, and N. M. Harrison, *New J. of Physics* **10**, 033002 (2008).
- V. M. Pereira, J. M. B. Lopes dos Santos, and A. H. Castro Neto, *Phys. Rev. B* **77**, 115109 (2008).
- J. J. Palacios, J. Fernandez-Rossier, and L. Brey, *Phys. Rev. B* **77**, 195428 (2008).
- O. V. Yazyev, *Phys. Rev. Lett.* **101**, 037203 (2008).
- M. Bonfanti, R. Martinazzo, G. F. Tantardini, and A. Ponti, in preparation (2008).
- G. Kresse and J. Hafner, *Phys. Rev. B* **49**, 14251 (1994).
- G. Kresse and J. Hafner, *Phys. Rev. B* **47**, 558 (1993).
- G. Kresse and J. Furthmüller, *Comput. Mat. Sci.* **6**, 15 (1996a).
- G. Kresse and J. Furthmüller, *Phys. Rev. B* **54**, 11169 (1996b).
- P. E. Blöchl, *Phys. Rev. B* **50**, 17953 (1994).
- G. Kresse and D. Joubert, *Phys. Rev. B* **59**, 1758 (1999).
- J. P. Perdew, K. Burke, and M. Ernzerhof, *Phys. Rev. Lett.* **77**, 3865 (1996).
- J. P. Perdew, K. Burke, and M. Ernzerhof, *Phys. Rev. Lett.* **78**, 1396 (1997).
- P. E. Blöchl, O. Jepsen, and O. K. Andersen, *Phys. Rev. B* **49**, 16223 (1994).
- M. Hasegawa and K. Nishidate, *Phys. Rev. B* **70**, 205431 (2004).
- H. Rydberg, N. Jacobsen, P. Hyldgaard, S. I. Simak, B. I. Lundqvist, and D. C. Langreth, *Surf. Sci.* **532-535**, 606 (2003).
- J. Kerwin and B. Jackson, *J. Chem. Phys.* **128**, 084702 (2008).
- Y. Ferro, F. Marinelli, and A. Allouche, *Chem. Phys. Lett.* **368**, 609 (2003).
- E. J. Duplock, M. Scheffler, and P. J. D. Lindan, *Phys. Rev. Lett.* **92**, 225502 (2004).
- T. Roman, W. A. Diño, H. Nakanishi, H. Kasai, T. Sugimoto, and K. Tange, *Carbon* **45**, 203 (2007).
- L. Chen, A. C. Cooper, G. P. Pez, and H. Cheng, *J. Phys. Chem. C* **111**, 18995 (2007).
- P. O. Lethinen, A. S. Foster, Y. Ma, A. V. Krasheninnikov, and R. M. Nieminen, *Phys. Rev. Lett.* **93**, 187202 (2004).
- M. Inui, S. A. Trugman, and E. Abrahams, *Phys. Rev. B* **49**, 3190 (1994).
- H. A. Mizes and J. S. Foster, *Science* **244**, 559 (1989).
- R. Ruffieux, O. Gröning, P. Schwaller, and L. Schlapbach, *Phys. Rev. Lett.* **84**, 4910 (2000).
- K. Kusakabe and M. Maruyama, *Phys. Rev. B* **67**, 2003 (2003).
- D. Jiang, B. G. Sumpter, and S. Dai, *J. Chem. Phys.* **124**, 124703 (2007).
- O. V. Yazyev, W. L. Wang, S. Meng, and E. Kaxiras, *Nano Lett.* **8**, 766 (2008).
- O. V. Yazyev and M. I. Katsnelson, *Phys. Rev. Lett.* **100**, 047209 (2008).
- M. Raimondi, M. Simonetta, and G. F. Tantardini, *Comp. Phys. Rep.* **2**, 171 (1985).
- D. L. Cooper, J. Gerratt, and M. Raimondi, in *Ab initio methods in quantum chemistry II*, edited by K. P. Lawley (John Wiley & Sons Ltd., 1987).
- J. Gerratt, D. L. Cooper, P. B. Karadakov, and M. Raimondi, *Chem. Soc. Rev.* **26**, 87 (1997).
- J. Li and R. McWeeny, *Int. J. of Quant. Chem.* **89**, 208 (2002).
- D. L. Cooper, *Valence Bond Theory - Theoretical and computational chemistry 10* (Elsevier, 2002).
- M. Simonetta, E. Gianinetti, and I. Vandoni, *J. Chem. Phys.* **48**, 1579 (1968).
- D. L. Cooper, J. Gerratt, and M. Raimondi, *Chemical Reviews* **91**, 929 (1991).
- G. F. Tantardini, M. Raimondi, and M. Simonetta, *J. Am. Chem. Soc.* **99**, 2913 (1977).
- D. L. Cooper, J. Gerratt, and M. Raimondi, *Nature* **323**, 699 (1986).
- J. Hubbard, *Proc. Roy. Soc. A* **276**, 238 (1963).
- J. Wu, T. G. Schmalz, and D. J. Klein, *J. Chem. Phys.* **117**, 9977 (2002).
- J. Wu, T. G. Schmalz, and D. J. Klein, *J. Chem. Phys.* **119**, 11011 (2003).
- R. Pariser and R. G. Parr, *J. Chem. Phys.* **21**, 466 (1953a).
- R. Pariser and R. G. Parr, *J. Chem. Phys.* **21**, 767 (1953b).
- J. A. Pople, *Trans. Faraday Soc.* **49**, 1375 (1953).
- E. H. Lieb, *Phys. Rev. Lett.* **62**, 1201 (1989).